Simulation of Water and Energy Fluxes in an Old-Growth Seasonal Temperate Rain Forest Using the Simultaneous Heat and Water (SHAW) Model

TIMOTHY E. LINK

Department of Forest Resources, University of Idaho, Moscow, Idaho

GERALD N. FLERCHINGER

Northwest Watershed Research Center, USDA Agricultural Research Service, Boise, Idaho

MIKE UNSWORTH

Department of Atmospheric Sciences, Oregon State University, Corvallis, Oregon

DANNY MARKS

Northwest Watershed Research Center, USDA Agricultural Research Service, Boise, Idaho

(Manuscript received 20 May 2003, in final form 31 December 2003)

ABSTRACT

In the Pacific Northwest (PNW), concern about the impacts of climate and land cover change on water resources and flood-generating processes emphasizes the need for a mechanistic understanding of the interactions between forest canopies and hydrologic processes. Detailed measurements during the 1999 and 2000 hydrologic years were used to modify the Simultaneous Heat and Water (SHAW) model for application in forested systems. Major changes to the model include improved representation of rainfall interception and stomatal conductance dynamics. The model was developed for the 1999 hydrologic year and tested for the 2000 hydrologic year without modification of the site parameters. The model effectively simulated throughfall, soil water content profiles, and shallow soil temperatures for both years. The largest discrepancies between soil moisture and temperature were observed during periods of discontinuous snow cover due to spatial variability that was not explicitly simulated by the model. Soil warming at bare locations was delayed until most of the snow cover ablated because of the large heat sink associated with the residual snow patches. During the summer, simulated transpiration decreased from a maximum monthly mean of 2.2 mm day^{-1} in July to 1.3 mm day^{-1} in September as a result of decreasing soil moisture and declining net radiation. The results indicate that a relatively simple representation of the vegetation canopy can accurately simulate seasonal hydrologic fluxes in this environment, except during periods of discontinuous snow cover.

1. Introduction

The transport of mass and energy in forest environments is important because of concerns about effects of climate on vegetation and about influences of forest management on floods, seasonal low flows, and geomorphic processes. Intensive, interdisciplinary field studies and complementary modeling programs have increased our understanding of the processes controlling mass and energy fluxes in forests (e.g., Sellers et al. 1997). Physically based models have greatly increased our understanding of the complex interactions between hydrologic processes and vegetation by providing tools for simulation, prediction, and hypothesis testing. The continued development of robust modeling tools is particularly important in regions such as the Pacific Northwest (PNW) of the United States, where competing demands on water and forest resources have raised many questions regarding the effects of land cover and climate variability on hydrologic systems.

In the PNW, disturbance of the native forest cover may contribute to increases in peak streamflows (Jones 2000; Jones and Grant 1996), although the magnitude of the increase, return interval of the affected peaks, and size of affected basins may vary (Bowling et al. 2000; Storck et al. 1998; Thomas and Megahan 1998). The PNW climate is characterized by an extended seasonal drought during summer, and questions about how land management influences the low flow regime have

Corresponding author address: Dr. Timothy E. Link, Department of Forest Resources, University of Idaho, P.O. Box 441133, Moscow, ID 83844-1133.
E-mail: tlink@uidaho.edu

recently increased with concerns about water resource availability and survival of endangered species (Keppeler and Ziemer 1990). The studies referenced above suggest that a variety of physical mechanisms associated with canopy alteration may affect streamflows; these include precipitation interception, transpiration, and alteration of snow cover and soil moisture regimes. Understanding how vegetation and hydrology interact is therefore necessary to distinguish the relative importance of these mechanisms.

Physically based numerical models are powerful tools to help understand interactions of vegetation and hydrology and to test hypotheses regarding the effects of land cover and climatic variability on hydrologic processes. Existing soil–plant–atmosphere models simulate a number of interrelated mass and energy transfer processes through layered soil–vegetation–atmosphere systems (e.g., Flerchinger et al. 1996b; Sellers et al. 1996; Wigmosta et al. 1994; Williams et al. 2001). Physically based models are commonly developed and validated in a particular environment and within a range of driving variables, but if limited validation data exist, plausible results may occur if counteracting and conflicting assumptions or errors are made when developing and/or determining site parameters for the model. The power and reliability of process models may be extended by fully testing and validating the processes simulated by models across a range of distinctly different environments and climate conditions.

This paper describes further development of the Simultaneous Heat and Water (SHAW) model, a one-dimensional hydrologic model that integrates the coupled transport of mass and energy through a soil–vegetation–atmosphere system into a simultaneous solution (Flerchinger et al. 1996b; Flerchinger and Saxton 1989). The model was developed and extensively validated over a variety of semiarid and arid cropland and rangeland vegetation covers. Many aspects of the model have been tested, including the effects of vegetation on soil temperature and moisture (Flerchinger and Pierson 1997), snowmelt (Flerchinger et al. 1996a; Flerchinger et al. 1994), soil freezing (Flerchinger and Saxton 1989), evapotranspiration and surface energy budgets (Flerchinger et al. 1996b), and radiometric surface temperature (Flerchinger et al. 1998). To date, the SHAW model has not been tested in humid forested environments, although the representation of the physics and vegetation structure in the model indicate that it could be effective in such environments.

The primary objective of this research was to develop the SHAW model for application in a seasonal temperate rain forest. Specifically, we 1) tested the model for a complete annual cycle in a PNW old-growth rain forest to encompass the full range of a single season's climate variability in the region; 2) validated the individual hydrologic processes and state variables simulated by the model, including snow-cover deposition and ablation, soil water content, soil temperatures, canopy interception losses, and transpiration fluxes; 3) tested the simulations for a year of independent data (i.e., data not used for developing the model); and 4) quantified the annual and monthly components of the site energy and water balances.

2. Methods

a. Site description

This study was conducted at the Wind River Canopy Crane Research Facility (WRCCRF), located within the T. T. Munger Research Natural Area of the Gifford Pinchot National Forest, in southwestern Washington. The site is located on a gently sloping alluvial fan in the Wind River Valley in the Cascade Mountains at 45°49′N latitude, 121°57′W longitude, at an elevation of 367.5 m MSL.

Dominant species at the site are Douglas fir (*Pseudotsuga menzesii*), western hemlock (*Tsuga heterophylla*), and western red cedar (*Thuja plicata*), with many individuals exceeding 450 yr in age and 60 m in height. Soils at the site consist of loamy sands and sandy loams characterized by low bulk densities and high porosities (see appendix) (Dyrness 2003). The physical setting, ecological characteristics, and infrastructure of the WRCCRF are described in detail by Shaw et al. (2004).

Climate at the site is characterized by cool, wet winters and warm, dry summers, with an average annual precipitation of 2467 mm (measured from 1931 to 1977). Less than 10% of the precipitation occurs between June and September (Shaw et al. 2004). Snowfall is most common from November to March and varies widely between years, because the site is located near the lower limit of the transient snow zone. Mean annual air temperature is 8.7°C, with the mean monthly maximum of 17.3°C occurring in August, and the mean monthly minimum of −0.1°C occurring in January. Annual precipitation during the 1999 and 2000 water years was 5% and 0% above the long-term average, respectively. The 1999 winter was warmer than average, and a greater proportion of the precipitation occurred as rain rather than snow, causing the development of a spatially discontinuous snow cover during this year. The 2000 winter temperatures were closer to average, producing a spatially continuous snow cover that persisted from mid-January through early April.

b. Data collection and instrumentation

An 85-m tower crane installed at the WRCCRF was used as a sensor platform for meteorological measurements. Meteorological data for driving the model were collected above the canopy at 85 m (STA80) and 68.4 m (STA70) on the crane tower and at an open field site (OPENSTA) approximately 1.5 km south of the crane tower. Validation data for soil water content (θ), soil

temperature (T_g), throughfall (P_n), and snow depth (z_{snow}) were collected throughout the 2.3-ha circle described by the crane boom rotation. Automated stations were also installed within a typical closed canopy area and within a forest gap to provide continuous measurements of θ, T_g, and z_{snow}.

1) METEOROLOGICAL DATA

Solar radiation (R_S) was collected at STA80 using a four-component net radiometer (Model CNR-1, Kipp and Zonen, Inc., Bohemia, New York). A combination air temperature (T_a) and relative humidity (RH) sensor (Model HMP35C, Vaisala, Inc., Sunnyvale, California) was installed at STA70 in a mechanically aspirated Gill multiplate radiation shield. Wind velocity was measured at STA70 with a three-dimensional sonic anemometer (Solent Gill HS, Lymington, United Kingdom). Gross precipitation (P_G) was measured above the canopy at STA80 with an alter-shielded weighing gauge (Model 6071, Belfort Instrument Co., Baltimore, Maryland) and at OPENSTA using both a weighing (Model 5-780, Belfort Instrument Co., Baltimore, Maryland) and a tipping bucket rain gauge (Model TE-525, Texas Electronics, Inc., Dallas, Texas).

2) VALIDATION DATA

Volumetric soil water content (θ) in the top 40 cm of the soil was measured every 3–4 weeks using time-domain reflectometry (TDR; Model Trase 6050XI, Soil Moisture Equipment, Inc., Santa Barbara, California). In the top 30 cm, θ was monitored continuously using four frequency reflectometers (CS615, Campbell Scientific, Inc., Logan, Utah). Water contents over depth intervals of 0–15, 15–30, 30–60, 60–90, and 90–120 cm were measured with segmented TDR probes (Type A, Environmental Sensors, Inc., San Diego, California), interrogated with a portable TDR unit (Model MP-917, Environmental Sensors, Inc., San Diego, California).

Soil temperatures at 15 cm were measured with thermistors (Model 107, Campbell Scientific, Inc., Logan, Utah). Soil temperatures between extremes of canopy cover were very similar during most of the year, and therefore averages of the probes were assumed to represent mean-site conditions.

Throughfall during snowfall-free periods was measured with an array of 44 bottle collectors during the 1999 water year and with an array of 24 tipping bucket rain gauges (TE-5251, Texas Electronics, Inc., Dallas, Texas) during the 2000 water year. Snow depths at the gap and closed sites were measured with sonic depth sensors (Judd Communications, Inc., Logan, Utah).

Ecosystem water flux (ET) was measured by an eddy covariance (EC) system mounted at 70 m on the crane tower, using a 3D sonic anemometer and a fast-response infrared gas analyzer (Model 6262, LiCor, Inc., Lincoln, Nebraska). Full details of the system, methods, and data corrections are given by Paw U et al. (2004). The source area contributing to the ET measurement (the footprint) extends typically less than 100 m upwind during unstable daytime conditions, but may extend more than 1 km upwind during stable conditions at night. Measurements were affected by the crane tower for wind directions in the quadrant 45°–135° and were therefore excluded from this analysis. Eddy covariance data were available for the period from 20 May 1998 through 31 July 1999 and from 4 January through 17 June 2000 at the time this analysis was completed.

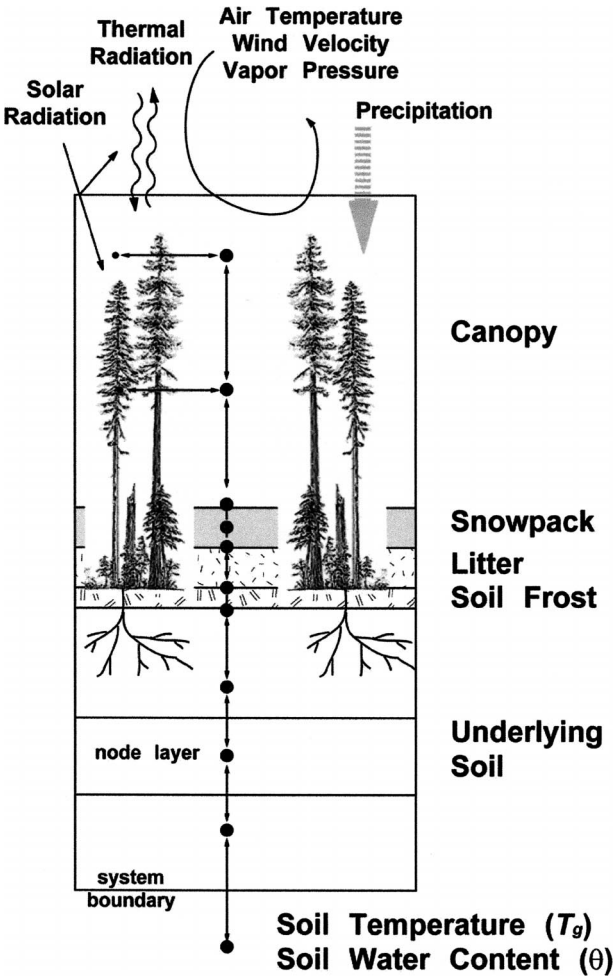

FIG. 1. Conceptual diagram of the SHAW model.

c. SHAW model developments

1) MODEL DESCRIPTION

The SHAW model simulates a vertical, one-dimensional system composed of a vegetation canopy, snow cover (if present), litter, and soil profile. A conceptual diagram of the model structure is shown in Fig. 1. The model integrates the detailed physics of interrelated mass and energy transfer through the multilayer system

into one simultaneous solution. Hourly predictions include evaporation, transpiration, snow depth, runoff, and profiles of soil water content and temperature.

Boundary conditions are defined by meteorological variables (R_S, T_a, RH, u, and P_G) above the canopy, and soil variables (θ and T_g) at the lower boundary. A layered system is established though the model domain, with each layer represented by a node. After computing fluxes at the upper boundary, the heat, liquid water, and vapor fluxes between layers are simulated. Heat and water fluxes through the system are computed simultaneously using implicit finite-difference equations that are solved iteratively using a Newton–Raphson procedure (Campbell 1985). The model can simulate transfer in canopies comprised of several different plant species, including standing dead material. Vegetation height, biomass, leaf area index (LAI), rooting depth, and leaf dimension through the year are specified by the user. Details of the numerical implementation of the SHAW model are presented in Flerchinger (2003), Flerchinger et al. (1996b, 1998), and Flerchinger and Saxton (1989).

In the following sections we describe how the model was modified to more accurately simulate forest environments under a wide range of meteorological conditions. The most significant changes were in the canopy rainfall interception and canopy conductance to water vapor transport (g_c).

2) Canopy rainfall interception

The two most important canopy parameters that control the rainfall interception process are the direct throughfall proportion (p) and canopy storage capacity per unit leaf area (S_c) (Gash 1979). Values for p and S_c of the WRCCRF canopy were derived from detailed analysis of canopy throughfall (Link 2001). Previous versions of the SHAW model assumed that p was identical to the canopy transmissivity for direct solar radiation, computed as an exponential function of LAI. The mean measured value of p for 43 storms in 2000 was 0.36, much larger than the estimated value of 0.013, based on LAI. Storage capacity in the previous version of the SHAW model was specified as 1.0 mm per unit LAI. Detailed throughfall measurements indicated that the mean canopy storage capacity at the WRCCRF was 3.32 mm, which corresponds to a value $S_c = 0.386$ mm per unit LAI. The changes in the parameters p and S_c increased the simulated throughfall and transpiration fluxes, particularly during the dry months, by simulating less interception, higher throughfall, and by decreasing the amount of time that the canopy remained wet after rain.

Snowfall interception was treated as identical to rainfall interception. Rapid release of intercepted snow by canopy unloading and meltwater drip was observed at the site, similar to observations from other maritime sites (Storck et al. 2002). Although the SHAW model does not explicitly consider the process of canopy unloading, conditions in this environment favor brief canopy residence times due to rapid melt and mass release of intercepted snow loads.

3) Canopy conductance model

The physicochemical and physiological processes that interact to control stomatal mechanics are complex and poorly understood (Nobel 1991). Stomatal conductance (g_s) is influenced by many factors, including vapor pressure deficit (δe), leaf temperature (T_l), solar radiation, soil water status, and CO_2 concentration within the stomates (Jarvis 1976; Ogink-Hendriks 1995; Stewart 1988). Two common models of g_s are the Jarvis–Stewart model, which estimates g_s as a function of the environmental variables δe, T_a (as a proxy for T_l), R_S, and θ, and the Ball–Berry model (Ball et al. 1987) that relates g_s to CO_2 assimilation and humidity.

The SHAW model does not include a carbon cycle; therefore, g_s is estimated from environmental conditions. In previous versions of the model, g_s was computed as

$$g_s = r_{s0}[1 + (\psi_l/\psi_c)^n]^{-1}, \quad (1)$$

where r_{s0} is stomatal resistance with no water stress, ψ_l is leaf water potential, ψ_c is a critical leaf water potential at which stomatal resistance is 2 times its minimum value, and n is an empirical coefficient (Campbell 1985). The estimate of g_s in Eq. (1) is strongly dependent on soil water status and weakly dependent on δe, T_a, and R_S, through their influence on T_l and ψ_l. Equation (1) functioned effectively for semiarid vegetation (Flerchinger et al. 1996b, 1998; Flerchinger and Pierson 1997) but is less likely to be applicable to forests, particularly during the transition from spring to summer conditions, when θ is large and large diurnal variations in T_a and δe occur. During this period, vegetation must adjust g_s to balance transpiration against the ability to take up water from the soil. The Jarvis–Stewart formulation is an effective technique to estimate the effect of all environmental variables on g_s; however, its full implementation requires the estimation of six parameters (e.g., Ogink-Hendriks 1995). The derivation of the Jarvis–Stewart parameters from natural sites can be confounded by correlations between environmental variables and by data that do not adequately fill the variable space. This may result in mutual parameter dependency during the fitting procedure, indicating that the model is overparameterized with respect to the available data (Ogink-Hendriks 1995). These data issues are significant in many environments such as the PNW because of the strong correlation between T_a and δe and a weaker correlation between θ and δe.

A simplified version of the Jarvis–Stewart model was added to the SHAW model to more effectively simulate water dynamics in forested systems while maintaining the relative simplicity of the model and parameter parsimony. The computed conductance from Eq. (1) is mul-

tiplied by a reduction factor (f) computed as a function of δe, defined as

$$f(\delta e) = K_{\delta e} + (1 - K_{\delta e})r^{\delta e/1000}, \quad (2)$$

where $K_{\delta e}$ is the maximum g_s reduction factor at high δe, and r is an empirical fitting parameter (modified from Ogink-Hendriks 1995). Because T_a and δe are strongly correlated, the effect of temperature is implicitly included in the model. Equation (2) more accurately reduces g_s early in the growing season, when θ is large. Later in the season when δe reaches maximum values and the system becomes increasingly limited by θ, computed g_s is further limited by Eq. (1). The effect of R_s on g_s is not included in the current model because we assume that when R_s is low, transpiration will be limited by low available energy and vapor gradients such that the net impact on the computed flux will be negligible.

d. Site parameter determination

Mass and energy dynamics were simulated for the 1999 and 2000 hydrologic years. The SHAW model is physically based and does not require calibration; however, a number of physical parameters describing the site are required. All parameters were derived from measurements at the site where possible, or estimated from literature values where no site data existed. The state variables used in the model were optimized by comparing simulation results to data collected during the 1999 development period. During the development year, parameter adjustments were limited to measured and estimated soil properties (specifically, K_{sat} and the pore-size distribution index) to more accurately simulate observed drainage trends. The parameters used in the 1999 simulations were subsequently applied without modification for the 2000 hydrologic year. The site parameters used in the simulations are listed in the appendix.

1) CANOPY CHARACTERISTICS

The canopy was modeled as 10 layers composed of a single species since much of the validation data (i.e., θ and ET) is at the stand scale and does not differentiate between species. Seasonal variations in the canopy structure are relatively small in conifer canopies; therefore, canopy characteristics were assumed to remain constant over time. The total LAI of the canopy was assumed to be 8.6, the value reported for the years 1997–99 (Thomas and Winner 2000). The clumping factor for radiation transmission was assumed to be 0.65 based on measured below-canopy radiation. Canopy biomass was estimated from a detailed canopy inventory using allometric techniques (Harmon et al. 2004). Rooting depth was estimated to be 1.2 m, with approximately 90% of the total biomass in the top 30 cm, based on minirhizotron measurements and from observation of soil cores and pits during this study.

Stomatal conductance parameters were derived from 30-min-averaged EC measurements of ET during the period from 20 May through 30 December 1998, obtained from the Ameriflux Web site (http://cdiac.esd.ornl.gov/ftp/ameriflux/data/us-sites/preliminary-data/-Wind-River/). The data were screened to extract periods where the canopy was dry, soil heat (G) and canopy storage (St) heat fluxes were negligible (i.e., between 1000 and 1400 h), and where transpiration was not expected to be limited by soil moisture (i.e., $\theta \geq 20\%$ vol vol^{-1}). The filtering procedure reduced the dataset to less than 6% of the original values (from 10 766 to 599 points) for the g_c analysis. The filtered flux data were used to derive g_c for each value by inverting the Penman–Monteith equation, assuming that the atmospheric conductance for water vapor was identical to the conductance for momentum, which was computed using the friction velocity measured by the EC system.

The maximum canopy conductance ($g_{c,\max}$), estimated by extrapolating the upper envelope of the computed g_c values to $\delta e = 0$ was 36 mm s^{-1}, which corresponds to a maximum average stomatal conductance of 4.2 mm s^{-1}, assuming an LAI of 8.6. The estimate of $g_{c,\max}$ is near the upper limit obtained from leaf-level measurements of stomatal conductance for tree species in general (Nobel 1991) and for Douglas fir (Bond and Kavanagh 1999).

Canopy conductance data derived from the ET flux measurements were converted to a relative canopy conductance (g_{rel}), defined as

$$g_{\text{rel}} = g_c/g_{c,\max}. \quad (3)$$

Parameters for the canopy conductance model were determined by fitting Eq. (2) to the approximate upper envelope of the g_{rel} versus δe data, as shown in Fig. 2.

2) LITTER AND SOIL PROPERTIES

The surface layer at the WRCCRF site is characterized by a thick litter layer of needles and fine woody debris that insulates the underlying mineral soil from heat transfer and intercepts a portion of the throughfall reaching the litter surface. The litter depth and mass per unit area were measured throughout the crane circle (Harmon et al. 2003), and all other parameters were estimated from values in the literature. The litter was represented in the model domain by six nodes.

Soil cores and excavations within the crane circle indicate that the soil profile is composed of three primary layers roughly corresponding to the A, B, and C horizons. The upper layer extends from the surface to 50 cm, a middle layer extends from 50 to 100 cm, and a very compact lower layer extends from approximately 100 cm to the lower boundary of the model domain at 200 cm (appendix). The bulk density, porosity, and water characteristic function from 0 to 15 bars were measured on 18 soil cores, collected in the upper 120 cm of the soil profile. Soil properties were similar to other analyses completed in the region that found low bulk densities ranging from ~0.8 to 1.1 g cm^{-3} and high

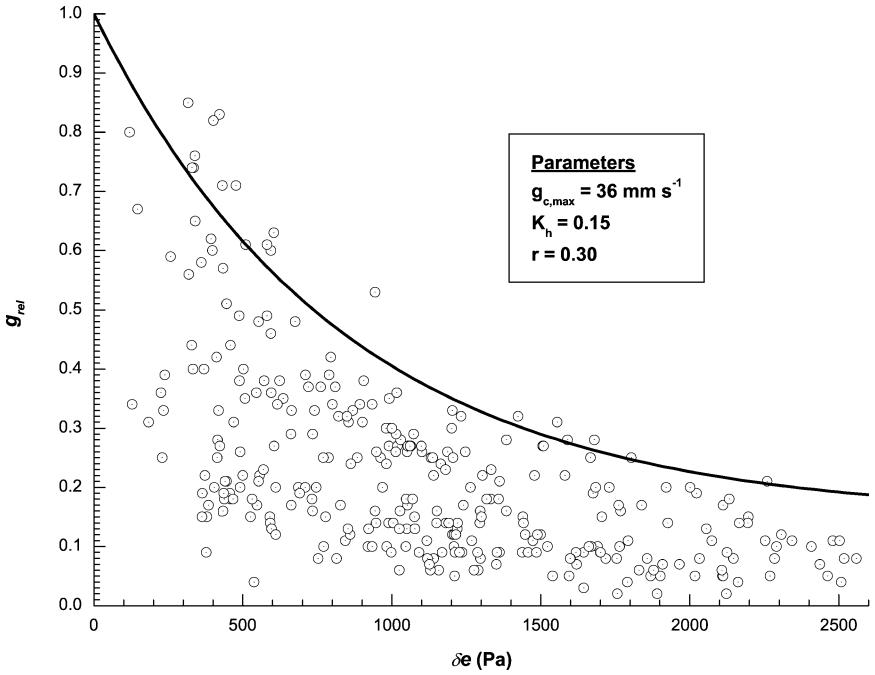

FIG. 2. Scatterplot of relative canopy conductance vs vapor pressure deficit. Individual data points were derived from EC measurements of total ecosystem water flux during the summer of 1998. The solid line is a plot of Eq. (2).

porosities ranging from 50% to 75% (Harmon et al. 2003). The analyses indicate that the upper portion of the profile to 100 cm drains relatively freely, whereas the lower compact layer retains relatively high water contents at high soil tensions (appendix).

The soil profile was represented by 24 nodes in the model domain. The SHAW model can effectively simulate soil processes with fewer nodes; however, the higher number was selected to provide a direct comparison to T_g and θ validation depths.

3. Results and discussion

The overall goal of this research was to simulate the seasonal variation in hydrologic processes occurring over the entire 2.3-ha crane circle; therefore, we assessed the model performance based on mean-site conditions. Near-surface conditions may be affected by overlying canopy properties, which influence interception of radiation and precipitation and may produce apparent errors because of differences in the sampling and modeling scales. Intrasite variability, such as litter depth and quality, soil properties, preferential flow paths, topographic position, and depth to groundwater may also introduce apparent errors. We did not expect perfect agreement between measured and modeled values but sought to reproduce the seasonal trends of fluxes and scalars.

a. Snow processes

Figures 3a and 3b show simulated and measured snow depths for the 1999 and 2000 winters. Simulated and measured snow water equivalent (SWE) values during the 2000 winter are presented in Table 1. Snow-cover properties (depth and density) at the WRCCRF site were observed to be extremely variable across the site; therefore, snowpack properties were measured at a large canopy gap and beneath a dense closed canopy location to record the relative extremes of snow conditions within the crane circle. A rigorous validation of the simulated snow cover requires detailed spatial and temporal measurements of SWE, density, temperature, and liquid water content. Detailed validation could not be completed with the limited data that were collected; therefore, we assess the ability of the model to simulate the general snow-cover trends observed at the site, assuming that the average snowpack properties at the site were between the two measured extremes.

In general, simulated snow depth values were within the range observed between the two measurement locations. Simulated depth trends generally matched the observed trends, with the exception of a gradually increasing simulated trend during February 2000. The differences between these trends are probably due to a combination of errors in the rain/snow threshold and in the snow densification function, which does not account for densification due to canopy unloading.

In both years, a simulated shallow snow cover ($<$10

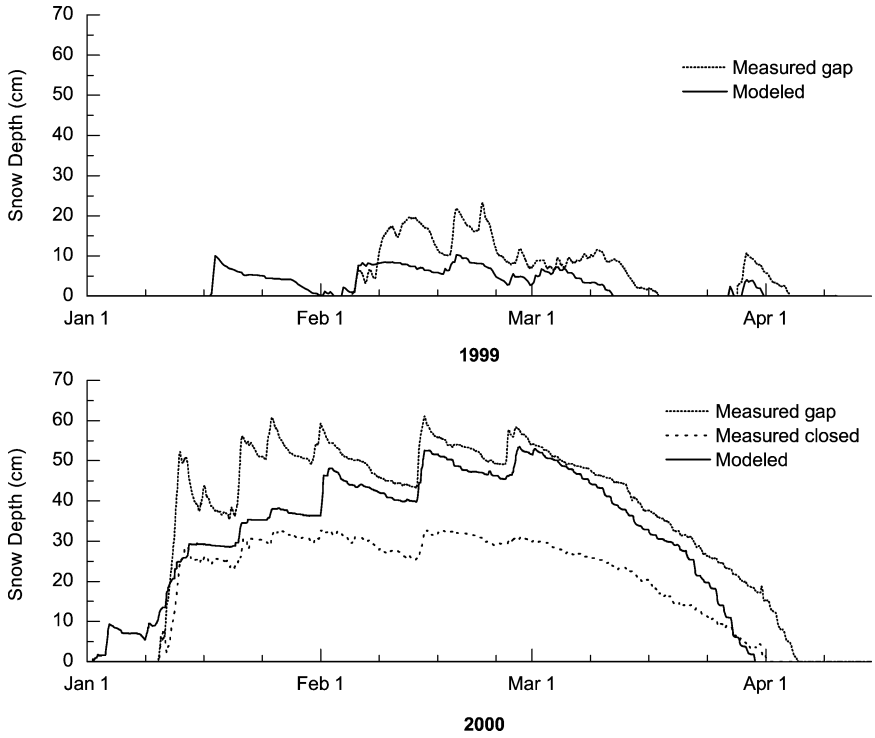

FIG. 3. Measured and modeled snow-cover depths. No snow was measured at the closed canopy site in 1999.

cm) developed 1–2 weeks prior to the observed development. Simulated ablation of the snow cover preceded measured ablation in the canopy gap by approximately 4–5 days during both simulation years. This result is not surprising since SWE was observed to be less in the closed canopy location, relative to the gap location. Simulated ablation also preceded measured ablation beneath the closed canopy location by 1–2 days in 2000, suggesting that the model slightly overestimates melt rates. SWE measurements during the development and ablation phases were slightly less than the measured SWE in the canopy gap, suggesting that the model is consistent in simulating the mass balance of the snowpack for the periods that data were collected.

Accurate simulation of snowpack dynamics under the observed meteorological conditions is particularly difficult because the simulation of the precipitation phase is controlled by T_a, which oscillates about the rain/snow threshold temperature. For example, although the rain/snow threshold at WRCCRF was estimated to be $\sim$1.3°C based on temperature, precipitation, and snow depth observations, rain and snow events at the site occurred on both sides of this threshold. This is consistent with other observations in the PNW that found mixed snow/rain and snow events occurring over a range of temperatures from $-1°$ to 3°C (U.S. Army Corps of Engineers 1956), indicating that slight variations in T_a and dewpoint temperature may produce errors in the simulated precipitation phase. Furthermore, the assumption of a continuous snow cover is invalid during these periods, which introduces error into the computation of snowmelt. Observed meltout discrepancies may also be due to measurement errors because the accuracy of sonic snow sensors declines for shallow snow covers ($<$15 cm) because of scattering of the signal by the nonuniform snow surface. Considering the wide range of snow-cover variability at the site, and the difficulty of accurately simulating snow covers that develop at temperatures near the rain/snow threshold, we considered the model performance to be reasonable for the general representation of snow-cover processes in this environment.

TABLE 1. Measured and modeled snow water equivalent, 2000.

Date	Measured (closed)	Measured (gap)	Modeled
27 Jan	164 mm	179 mm	173 mm
8 Mar	nd*	225 mm	220 mm

* Here nd = no data. On 8 Mar the snow cover under closed canopy areas consisted of thick ice layers that could not be sampled with a standard snow density cutter.

b. Throughfall

Cumulative gross precipitation and measured and modeled cumulative throughfall for the 2000 rainfall season are shown in Fig. 4. Figure 4 indicates that although the throughfall for individual events may be

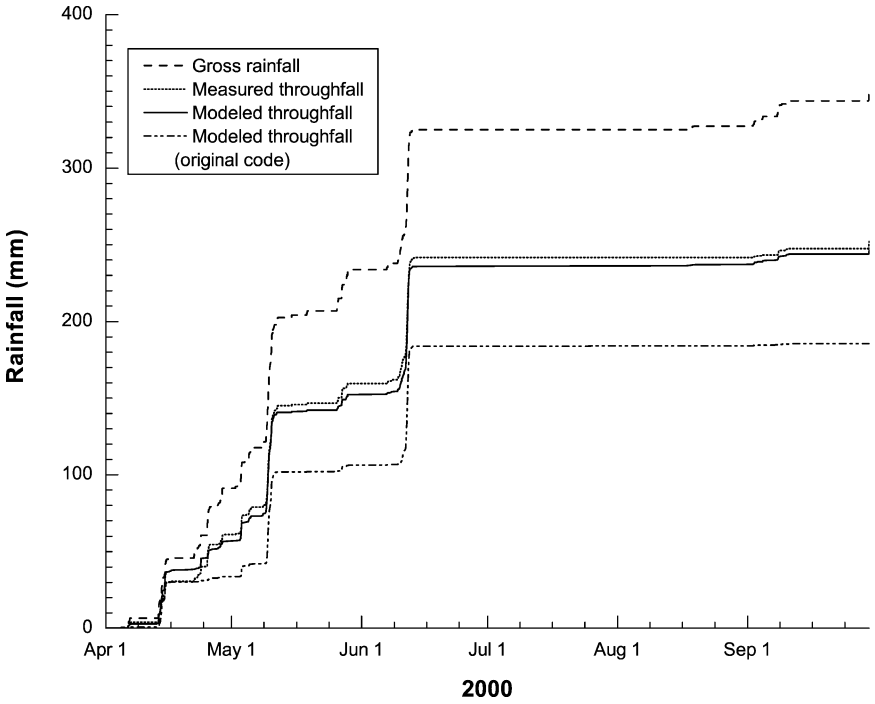

FIG. 4. Measured and modeled cumulative rainfall and throughfall for 2000.

over- or underestimated by the model, the temporal throughfall trends are generally well represented. Also shown are results of a simulation completed with the original model code, indicating that modified canopy parameters greatly improve the simulation of throughfall.

Table 2 presents the total precipitation (P_G), throughfall (P_n), and interception losses (E_i) for the 1999 and 2000 measurement periods. Simulated throughfall results spanned the snow-free measurement periods during the 1999/2000 and 2000/01 water years for direct comparison to the measured data. Simulated net throughfall closely matched the measured results as indicated by small (<4%) differences between measured and simulated P_n and E_i. The throughfall validation in 2000 suggests that the application of the mean canopy throughfall parameters are effective for computing long-term rainfall interception dynamics with the SHAW model.

TABLE 2. Throughfall and interception summary.

Precipitation component	Throughfall measurement period	
	8 Apr–8 Nov 1999	30 Mar–3 Dec 2000
P_G (mm)	451	619
Measured P_n (mm)	348	464
Modeled P_n (mm)	351	469
Difference (%)	0.7	1.1
Measured E_i (mm)	103	155
Modeled E_i (mm)	100	150
Difference (%)	−2.5	−3.4

c. Soil water content

Results of soil water content simulations are presented in Figs. 5a and 5b for the 1999 and 2000 hydrologic years, respectively. The average 0–30-cm θ is compared with measurements from an automated sensor that was found to track the average site soil water contents (Link 2001). Also shown for 1999 are results using the g_s parameterization in the original version of the SHAW model, but with the improved interception parameterization, to illustrate the specific impact of the new modification. Results of simulations of θ at greater depths are shown in Figs. 6a and 6b. Midwinter measurements of deep θ using the segmented probes could not be completed during the winter of 2000 because of snow cover.

Model performance is assessed using the Nash–Sutcliffe coefficient, or model efficiency (ME), root-mean-square difference (RMSD), and absolute mean bias difference (AMBD), defined in Table 3. Model performance statistics used to evaluate the simulations of θ in the 0–30-cm layer are presented in Table 4.

The ME for θ in the 0–30-cm layer was 0.88 and 0.91 for the 2 yr, indicating that the model reasonably simulated the water content dynamics at the site. RMSDs for the 2 yr were slightly greater than 2% vol vol^{-1}, with AMBDs less than 1% vol vol^{-1}. The modeled differences were well within the measurement error and were much less than the spatial variability observed within the site (Link 2001). Performance statistics were slightly better for 2000, probably due to greater errors

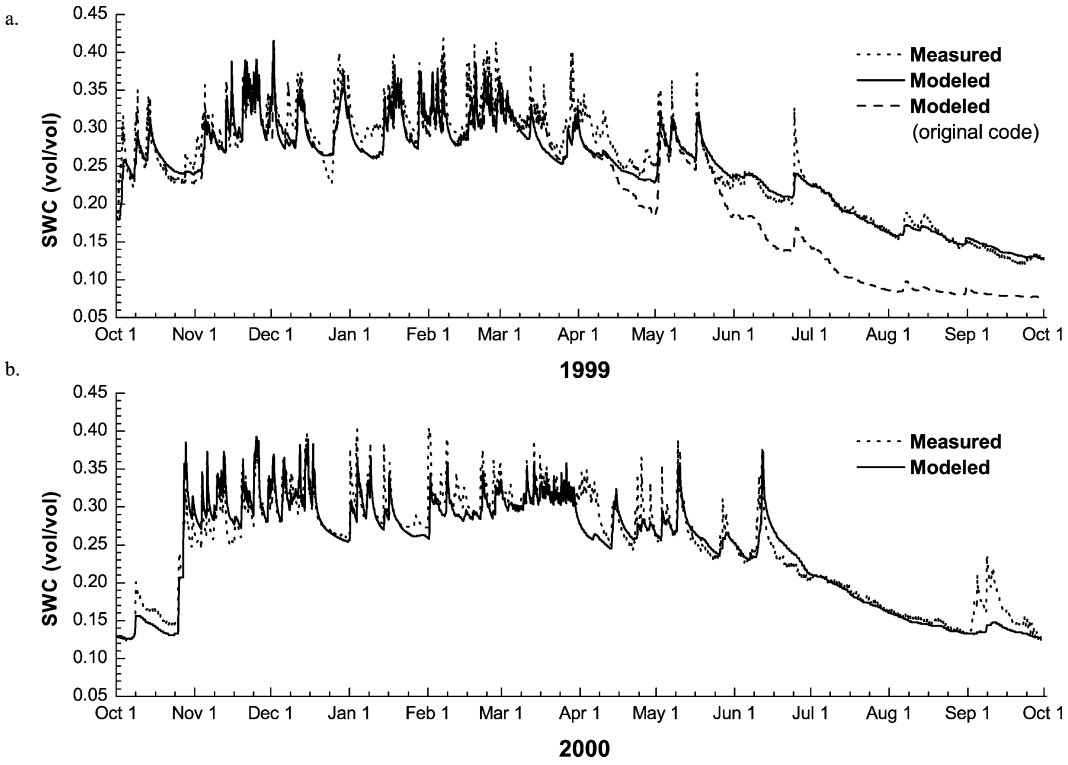

FIG. 5. Measured and modeled 0–30-cm soil water content for (a) 1999 and (b) 2000.

in the simulated snow-cover deposition and ablation that occurred during the warmer 1999 winter, when there was a transient and discontinuous snow cover. In contrast, the results from the simulation using the original g_s parameterization [Eq. (1)] show how the model performance was reduced if the environmental feedback between δe and g_s was neglected.

The largest differences between the measured and modeled values of θ occurred during the late winter months because of errors in the simulation of the timing and rate of snow-cover deposition and ablation. A large degree of spatial variation in the subcanopy snow cover was observed during these periods owing to variations in canopy interception, so these modeling differences are not surprising when using data from a proxy sensor to validate stand-level simulations. The simulated response of θ to precipitation events was often less than the measured response, probably because the model simulates mean-site canopy conditions, whereas the proxy measurement was made in a canopy gap with greater throughfall. This is particularly evident during a series of events in September 2000 when the seasonal soil moisture wetting phase begins.

Simulations of θ at greater depths were validated against periodic measurements of θ with the segmented moisture probes and are shown in Figs. 6a and 6b. The measured and modeled θ for the 60–90- and 90–120-cm soil layers exhibited reasonable agreement for both years. The simulated θ of the 30–60-cm layer was consistently about 5% vol vol^{-1} higher than the measured values during the winter months but showed good agreement during the summer drydown period.

d. Soil temperature

Figures 7a and 7b show simulations of soil temperature at 15 cm; model-fitting statistics are included in Table 4. The model accurately simulated T_g during both years, as indicated by high MEs of 0.99 to 0.98, RMSDs less than 1°C, and a negligible (<0.2°C) bias throughout the year. Model performance for 2000 was very similar to 1999, indicating that the selected parameters were also effective for simulated soil heat dynamics.

During the 1999 winter, when the snow cover was transient and discontinuous, simulated T_g departed from the measurements. In 2000, when there was a deeper, continuous snow cover, soils maintained a low and relatively constant temperature through the winter, followed by a rapid rise after the snow cover ablated. Comparison between the 2 yr showed the pronounced effect of the seasonal snow cover on the soil temperature regime and timing of soil warming. An understanding of snow-cover dynamics is therefore critical to understand the timing of soil warming and the onset of biologically controlled processes such as transpiration and respiration.

The largest differences between the measured and modeled T_g also occurred during the early and late win-

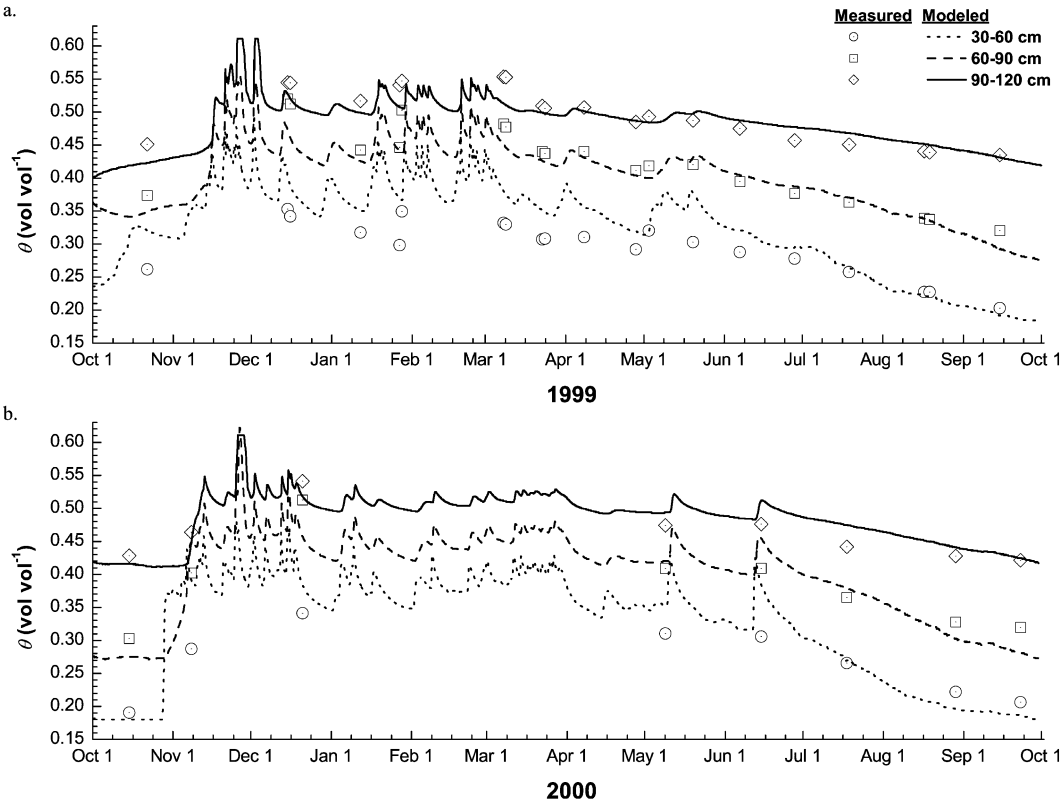

FIG. 6. Measured and modeled deep soil water content for (a) 1999 and (b) 2000. Midwinter measurements could not be completed in water year 2000 because of the development of a continuous snow cover that restricted access to TDR probes.

ter months due to slight errors in either the timing and/or the spatial distribution of the below-canopy snow cover. When the simulations predicted that snow cover had disappeared toward the end of March 2000, simulated T_g increased rapidly (Fig. 7b). However, when the actual snow cover over a T_g sensor ablated, but large quantities of snow remained in other areas of the site, soil warming was suppressed because the existing snow acted as a heat sink, preventing the within-canopy air temperature from increasing. The discrepancy that occurred during late February–early March in 1999 was another example of this phenomenon. After most of the snow beneath the canopy ablated, simulated T_g trends closely matched the measured trends. In both simulations, the timing of the seasonal T_g increase was well represented, with simulated values at 15 cm exceeding 3°C only 5 days prior to the measured date. Further improvement of the canopy mass and energy transfer formulations could improve the simulated timing of snow-cover ablation and soil warming but would probably add complexity to the model.

TABLE 3. Model performance statistics, where n is the total number of observations, x_{obs} is the observed quantity at a given time step, x_{sim} is the simulated quantity at a given time step, and x_{avg} is the mean of the observed values.

Statistic	Equation	
ME	$\mathrm{ME} = 1 - \left[\frac{\sum_{i=1}^{n}(x_{obs} - x_{sim})^2}{\sum_{i=1}^{n}(x_{obs} - x_{avg})^2}\right]$	(4)
RMSD	$\mathrm{RMSD} = \frac{1}{n}\sqrt{\sum_{i=1}^{n}(x_{sim} - x_{obs})^2}$	(5)
AMBD	$\mathrm{AMBD} = \frac{1}{n}\sum_{i=1}^{n}(x_{sim} - x_{obs})$	(6)

e. Evaporation and transpiration

A comparison between simulated and measured diurnal ET trends is presented in Figs. 8a–c. The diurnal

TABLE 4. Model fitting statistics.

	1999		2000	
Parameter	θ (0–30 cm)	T_g (15 cm)	θ (0–30 cm)	T_g (15 cm)
ME	0.88	0.99	0.91	0.98
RMSD	2.1 vol vol^{-1}	0.6°C	2.1 vol vol^{-1}	0.6°C
AMBD	0.8 vol vol^{-1}	0.1°C	0.6 vol vol^{-1}	0.2°C
RMBD*	3.4%	—	2.3%	—
Mean	25.0 vol vol^{-1}	7.1°C	24.4 vol vol^{-1}	7.6°C

* Relative mean bias difference.

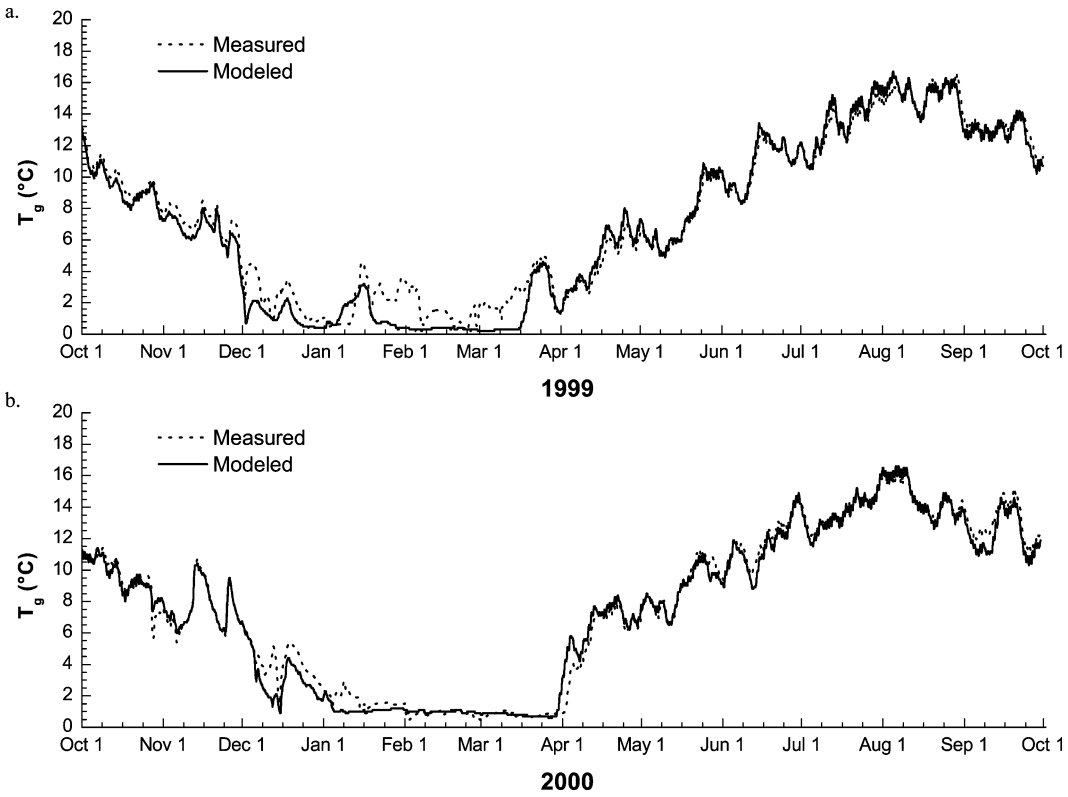

FIG. 7. Measured and modeled 15-cm soil temperature trends for (a) 1999 and (b) 2000. The largest differences between the measured and modeled values are related to spatial variation or simulation errors in the timing of snow-cover deposition and ablation.

trends in Figs. 8a and 8b represent ensemble-averaged fluxes for an 11- and a 17-day period in June and July, respectively, to correspond to the periods analyzed by Unsworth et al. (2004). Figure 8c shows the diurnal trend for a 9-day period in June 2000 to test model performance outside of the development year. The selected periods were characterized by dry conditions when evaporation from litter and soil was small; therefore, the fluxes are considered to be transpiration, appropriate for validating simulated transpiration by the SHAW model.

Modeled fluxes during the June and July 1999 periods matched the general pattern of the measured fluxes with a simulated hourly maximum of 0.22 mm h^{-1}, compared to the EC-measured maximum of 0.24 mm h^{-1}. During the July period, simulated maximum hourly ET fluxes were 0.33 mm h^{-1}, which closely matched the measured maximum of 0.30 mm h^{-1}. In the 2000 period, maximum measured water flux rates were 0.27 mm h^{-1} and preceded maximum simulated flux rates of 0.22 mm h^{-1} by approximately 2 h. The largest differences occurred in the morning and afternoon periods when measured fluxes were larger. The rapid increase in the measured flux in the morning can probably be attributed to transpiration of stored water within the stems of vegetation, which is not explicitly represented in the model. The rapid decline in simulated ET flux rates in the afternoon may be due to errors in the g_s parameterization or to a differing response of stomata to environmental conditions during the 1998 period from which g_s model parameters were derived.

Modeled and estimated ET for the ensemble periods are presented in Table 5. The simulated mean daily ET flux was 9% less, 5% greater, and 5% less than the EC mean daily evaporative flux for the June 1999, July 1999, and May–June 2000 periods, respectively. Several possible sources of error may contribute to the observed discrepancy between the EC and simulated ET fluxes. The SHAW model used measurements of local variables to simulate fluxes at a point assumed to be representative of the 2.3-ha plot. In contrast, the areal footprint sampled by the EC system is larger and varies in size, shape, and location depending on the wind velocity and direction (Baldocchi 1997; Lee 1998), and therefore EC-measured fluxes may differ from the point simulation. Additional sources of error may include advected moisture fluxes not measured by the EC system and assumptions that the microclimate data collected over a small canopy clearing is truly representative of above-canopy conditions. Considering the good agreement between the measured and simulated ET, and potential sources of error due to measurement methods and scales, we conclude that the SHAW model effectively simulated transpiration in this environment.

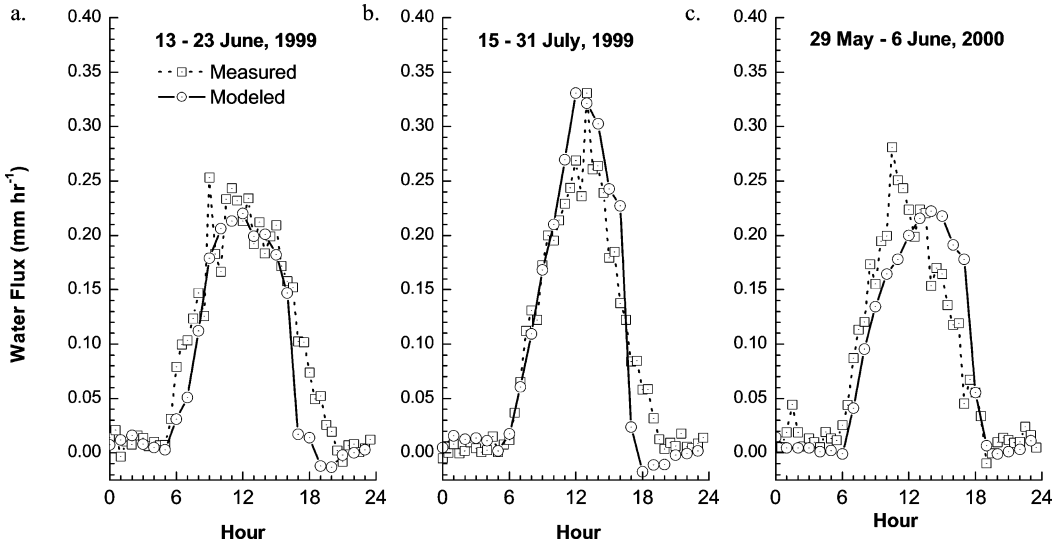

FIG. 8. Measured and simulated ensemble-averaged total ecosystem water fluxes for (a) 13–23 Jun 1999, (b) 15–31 Jul 1999, and (c) 29 May–6 Jun 2000.

f. Simulated energy and water fluxes

Based on the accurate simulation of soil moisture, temperature, rainfall interception, and transpiration at the seasonal scale, and reasonable general representation of snow-cover dynamics, we therefore assumed that modeled seasonal variations in energy and water fluxes are accurate for the 1999 and 2000 hydrologic years.

Table 6 contains a summary of simulated mean monthly net radiation (R_n), sensible (H), latent (λE), canopy storage plus soil (St + G) heat fluxes and the Bowen ratio (β) for the 1999 and 2000 hydrologic years. Sums of monthly precipitation and simulated evaporation, transpiration, runoff, and Δ storage are presented in Table 7. Positive values indicate fluxes toward the surface, and negative values indicate fluxes away from the surface. The shift from positive to negative H occurred between February and March in 1999 and between March and April in 2000. Latent fluxes were negative for all months, except for December 1998, which was characterized by anomalously cold conditions. In 1999, β was variable in the spring, but decreased from June through September. The spring months with higher Bowen ratios occurred during periods of relatively low precipitation, which resulted in smaller interception losses, and hence lower λE. In 2000, β increased steadily from April to July and decreased from July through September. It could be expected that β would increase through the summer drought period as T_a increased and the vegetation became increasingly water limited. However, as the dry season progressed, the climate at the WRCCRF became more continental as δe and climatic demand for evaporation increased. Despite the relatively dry soil conditions, the system was able to consistently

TABLE 5. Mean daily evapotranspiration results (mm day^{-1}).

Ensemble period	Modeled ET	Measured ET*
13–23 Jun 1999	1.8	2.0
15–31 Jul 1999	2.3	2.2
29 May–6 Jun 2000	1.9	2.0

* Measured by eddy covariance.

TABLE 6. Simulated mean monthly energy flux summary. Note that the sign convention for fluxes is that negative values correspond to trasfer from the surface to the atmosphere.

Hydrologic year	Month	R_n (W m^{-2})	H (W m^{-2})	λE (W m^{-2})	St + G (W m^{-2})	β
1999	Oct	35	4	−40	1	−0.10
	Nov	13	11	−21	−2	−0.52
	Dec	0	32	5	−36	6.4
	Jan	7	53	−21	−38	−2.52
	Feb	22	62	−33	−51	−1.88
	Mar	68	−12	−47	−9	0.26
	Apr	136	−88	−52	5	1.69
	May	165	−95	−83	13	1.14
	Jun	168	−108	−64	4	1.69
	Jul	206	−117	−85	−4	1.38
	Aug	155	−78	−76	−2	1.03
	Sep	115	−52	−61	−2	0.85
	Total	91	−33	−48	−10	0.69
2000	Oct	39	11	−40	−11	−0.28
	Nov	12	22	−22	−12	−1.00
	Dec	1	24	−7	−18	−3.43
	Jan	8	48	−29	−27	−1.66
	Feb	24	46	−38	−32	−1.21
	Mar	74	27	−60	−42	−0.45
	Apr	128	−39	−81	−8	0.48
	May	163	−57	−91	−15	0.63
	Jun	196	−86	−96	−14	0.90
	Jul	203	−116	−84	−4	1.38
	Aug	183	−95	−85	−2	1.12
	Sep	107	−36	−60	−11	0.60
	Total	95	−21	−58	−16	0.36

TABLE 7. SHAW monthly water flux summary.

Hydrologic year	Month	Precipitation (mm)	Evaporation (mm)	Transpiration (mm)	Drainage (mm)	Δ Storage (mm)
1999	Oct	95	23	11	0	61
	Nov	615	17	0	393	207
	Dec	526	−2	0	576	−43
	Jan	359	17	0	310	32
	Feb	621	22	0	550	48
	Mar	168	30	8	231	−94
	Apr	23	15	28	54	−74
	May	131	39	32	42	19
	Jun	28	16	37	17	−42
	Jul	5	6	66	4	−71
	Aug	23	16	49	0	−42
	Sep	3	5	46	0	−47
	Total	2596	205	278	2176	−48
2000	Oct	175	17	17	0	142
	Nov	569	17	1	370	181
	Dec	451	6	0	538	−90
	Jan	372	21	0	180	172
	Feb	337	25	1	156	154
	Mar	166	38	8	387	−262
	Apr	95	40	28	87	−59
	May	139	45	33	83	−22
	Jun	100	20	60	48	−26
	Jul	0	4	68	12	−83
	Aug	3	4	69	0	−70
	Sep	24	15	35	0	−28
	Total	2431	252	320	1860	9

transpire water under late summer conditions, probably because deep roots could access water, hence β decreased. If the system were more water limited and greater stomatal closure occurred, β would decrease at a slower rate, or might increase as observed in more arid canopies (Anthoni et al. 2002). These findings were consistent with comparisons of Bowen ratios between coniferous forests across a gradient from humid marine to continental environments (Jarvis et al. 1976; Wilson et al. 2002).

Water flow out of the system consisted almost entirely of evaporation, transpiration, and deep drainage from the soil profile. Surface runoff only occurred during an uncommon soil freezing event from 19 to 30 December 1998. Simulated drainage ceased only during August through October during both years. Net water storage in the system occurred in October and November when the soil profile rewetted after the summer drydown, and during midwinter months when the transient snow cover developed. The monthly water flux summary indicates that simulated ET was 18.6% and 23.5% of P_G during the 1999 and 2000 hydrologic years, respectively. Ecosystem water flux exceeded the monthly P_G during the months of April and June through September in 1999 and from July through September in 2000. During these months, transpiration decreased from an average maximum of 2.3 mm day^{-1} in July to a minimum of 1.3 mm day^{-1} in September.

The summary of the water balance components shows how the system shifted from a water surplus to a water deficit between May and June. The timing of the transition from water surplus to water deficit is particularly important because it controls the amount of time that vegetation is dependent on stored soil water to meet evaporative demands. The timing and magnitude of midsummer storms may also be an important source of water available for root uptake; however, the storms must be of sufficient size and/or frequency to fully saturate the canopy and litter layer and result in infiltration into the soil.

The SHAW model is a powerful tool that can be used to investigate the impacts of climate variability and canopy characteristics on individual hydrologic processes and on the seasonal variations of water and energy fluxes. The snow-cover transition zone is particularly sensitive to climatic variation because small increases in T_a will shift the system from a winter snow-dominated to rain-dominated regime, as exemplified by the 1999 winter. Similarly, shifts in the seasonal transition from wet to dry conditions may result in late-season reductions in transpiration as a result of alterations in the onset of the seasonal drydown. Future research directions will use the current site parameters with perturbed climate data to investigate how hydrologic fluxes might be expected to change in this system as a result of climatic shifts.

4. Summary and conclusions

Modifications to the SHAW model were presented for application in an old-growth seasonal temperate rainforest. Validation of individual hydrologic and physical processes simulated by the model exhibited reasonable agreement with measured values considering the potential sources of measurement error. Performance of the modified model was very similar for the 1999 development period and for the 2000 hydrologic year. Hydrologic processes in this system can be reasonably simulated by assuming that all trees have similar physiological characteristics and have static biophysical properties (e.g., LAI, rooting depth) throughout a seasonal cycle.

The process study presented here focused on a particular old-growth forest, whereas the PNW region contains forests of a wide range of canopy ages and conditions. Testing of the modified SHAW model in other forest systems is needed to test the generality of the model for application in other environments. Further testing of the model in forests where detailed spatial and temporal measurements of snow-cover properties exist is particularly needed to fully validate the simulated snow-cover processes. Additional studies focusing on detailed measurements and modeling of hydrologic processes in other canopy types are needed to develop an improved understanding of how mass and energy fluxes will respond to the coupled climate and vegetation variations in the PNW.

Acknowledgments. Support for this research was provided by the Office of Science, Biological and Environmental Research Program (BER), U.S. Department of Energy, through the Western Regional Center (WESTGEC) of the National Institute for Global Environmental Change (NIGEC) under Cooperative Agreement DE-FC03-90ER61010. Additional support was provided by the USDA Forest Service and the Agricultural Research Service, Northwest Watershed Research Center. Meteorological data were collected by the WRCCRF, which is a cooperative educational and scientific venture located on the Wind River Experimental Forest and supported by the University of Washington College of Forest Resources, the USDA Forest Service Pacific Northwest Research Station, and the Gifford Pinchot National Forest. Office and computing facilities were provided by the U.S. Environmental Protection Agency, Western Ecology Division. Eddy covariance data were provided by Matthias Falk and Dr. Kyaw Tha Paw U (University of California, Davis). The authors would like to thank Dr. Kelly Elder and three anonymous reviewers for helpful comments and suggestions.

APPENDIX
SHAW Model Site Parameters

Parameter definition	Value	Unit
Site properties		
Site lat	45, 49	degrees, min
Site lon	−121, 57	degrees, min
Site slope	6	%
Site aspect	45	degrees
Site elev	367.5	m
Time of solar noon	12.25	h
No. of plant species	1	
Measurement height	68	m
No. of canopy nodes	11	
No. of residue nodes	6	
No. of soil nodes	24	
Vegetation properties		
Height of species[a]	60	m
Characteristic dimension of leaves[b]	0.5	cm
Dry biomass of canopy[c]	30.7	kg m^{2}
Leaf area index[a]	8.6	m^{2} m^{-2}
Rooting depth[d]	1.2	m
Albedo of species[b]	0.25	Dimensionless
Transpiration threshold[b]	3.0	°C
Min stomatal resistance[d]	240	s m^{-1}
Resistance function exponent[b]	2	Dimensionless
Critical leaf water potential[b]	−150	m
Leaf resistance[b]	3.28×10^{4}	kg m^{-3} s^{-1}
Root resistance[b]	6.60×10^{4}	kg m^{-3} s^{-1}
Snow properties		
Maximum temperature for snow[b]	1.3	°C
Roughness length[b]	0.15	cm
Residue properties		
Fraction of surface covered[b]	1.0	
Albedo of residue[b]	0.20	Dimensionless
Dry mass of residue[c]	9000	kg ha^{-1}
Thickness of residue[b]	6	cm
Residue resistance to vapor transport[b]	50 000	s m^{-1}

Soil properties	Layer 1	Layer 2	Layer 3
Depth of layer[d] (cm)	0–50	50–100	100–200
Bulk density[d] (kg m^{-3})	800	800	1000
θ_{sat}[d] (vol vol^{-1})	0.5	0.65	0.65
Sand/silt/clay/organic matter[b]	20/70/10/15	20/70/10/15	25/65/10/3
K_{sat}[b] (cm h^{-1})	40	40	10
Ψ_e[d] (cm)	−0.02	−0.02	−0.03
Pore-size distribution index[d]	6.0	7.0	15

[a] Thomas and Winner (2000).
[b] Estimated.
[c] Harmon et al (2004).
[d] Measured, this study.

REFERENCES

Anthoni, P., M. H. Unsworth, B. E. Law, J. Irvine, D. D. Baldocchi, S. V. Tuyl, and D. Moore, 2002: Seasonal differences in carbon and water vapor exchange in young and old-growth ponderosa pine ecosystems. *Agric. For. Meteor.,* **111,** 203–222.

Baldocchi, D., 1997: Flux footprints within and over forest canopies. *Bound.-Layer Meteor.,* **85,** 273–292.

Ball, J. T., I. E. Woodrow, and J. A. Berry, 1987: A model predicting stomatal conductance and its contribution to the control of photosynthesis under different environmental conditions. *Progress in Photosynthesis Research,* J. Biggins, Ed., Martinus Nijhoff, 221–224.

Bond, B. J., and K. L. Kavanagh, 1999: Stomatal behavior of four woody species in relation to leaf-specific hydraulic conductance and threshold water potential. *Tree Physiol.,* **19,** 503–510.

Bowling, L. C., P. Storck, and D. Lettenmaier, 2000: Hydrologic effects of logging in western Washington, United States. *Water Resour. Res.,* **36,** 3223–3240.

Campbell, G. S., 1985: *Soil Physics with BASIC: Transport Models for Soil-Plant Systems.* Vol. 14, *Developments in Soil Science,* Elsevier, 150 pp.

Dyrness, C. T., cited 2003: Soil descriptions and data for soil profiles in the Andrews Experimental Forest, selected reference stands, RNA's, and National Parks: Long-Term Ecological Research. Forest Science Data Bank, Corvallis, OR, SP001. [Available online at http://www.fsl.orst.edu/lter/data/abstract.cfm?dbcode=SP001.]

Flerchinger, G. N., cited 2003: The Simultaneous Heat and Water (SHAW) model: User's manual. [Available online at ftp://ftp.nwrc.ars.usda.gov/download/shaw/SHAWUsersManual.pdf.]

——, and K. E. Saxton, 1989: Simultaneous heat and water model of a freezing snow–residue–soil system. I. Theory and development. *Trans. ASAE,* **32,** 565–571.

——, and F. B. Pierson, 1997: Modelling plant canopy effects on variability of soil temperature and water: Model calibration and validation. *J. Arid Environ.,* **35,** 641–653.

——, K. R. Cooley, and Y. Deng, 1994: Impacts of spatially and temporally varying snowmelt on subsurface flow in a mountainous watershed: 1. Snowmelt simulation. *Hydrol. Sci. J.,* **39,** 507–520.

——, J. M. Baker, and E. J. A. Spaans, 1996a: A test of the radiative energy balance of the SHAW model for snowcover. *Hydrol. Processes,* **10,** 1359–1367.

——, C. L. Hanson, and J. R. Wight, 1996b: Modeling evapotranspiration and surface energy budgets across a watershed. *Water Resour. Res.,* **32,** 2539–2548.

——, W. P. Kustas, and M. A. Weltz, 1998: Simulating surface energy fluxes and radiometric surface temperatures for two arid vegetation communities using the SHAW model. *J. Appl. Meteor.,* **37,** 449–460.

Gash, J. H. C., 1979: An analytical model of rainfall interception by forests. *Quart. J. Roy. Meteor. Soc.,* **105,** 43–55.

Harmon, M. E., and Coauthors, cited 2003: Permanent plots surrounding the Wind River Canopy Crane. Permanent Plots of the Pacific Northwest, Rep. 1. [Available online at http://www.fsl.orst.edu/lter/pubs/webdocs/reports/permplot/windriv.htm.]

——, K. Bible, M. J. Ryan, D. Shaw, H. Chen, J. Klopatek, and X. Li, 2004: Production, respiration, and overall carbon balance in an old-growth Pseudotsuga/Tsuga forest ecosystem. *Ecosystems,* in press.

Jarvis, P. G., 1976: The interpretation of the variations in leaf water potential and stomatal conductance found in canopies in the field. *Philos. Trans. Roy. Soc. London,* **B273,** 593–610.

——, G. B. James, and J. J. Landsberg, 1976: Coniferous forest. *Case Studies,* Vol. 2, *Vegetation and the Atmosphere,* 2d ed. J. L. Monteith, Ed., Academic Press, 171–240.

Jones, J. A., 2000: Hydrologic processes and peak discharge response to forest removal, regrowth, and roads in 10 small experimental basins, western Cascades, Oregon. *Water. Resour. Res.,* **36,** 2621–2642.

——, and G. E. Grant, 1996: Peak flow responses to clear-cutting and roads in small and large basins, western Cascades, Oregon. *Water. Resour. Res.,* **32,** 959–974.

Keppeler, E. T., and R. R. Ziemer, 1990: Logging effects on streamflow: Water yield and summer low flows at Caspar Creek in northwestern California. *Water. Resour. Res.,* **26,** 1669–1679.

Lee, X., 1998: On micrometeorological observations of surface–air exchange over tall vegetation. *Agric. For. Meteor.,* **91,** 39–49.

Link, T. E., 2001: The water and energy dynamics of an old growth-seasonal temperate rainforest. Ph.D. dissertation, Oregon State University, 169 pp.

Nobel, P. S., 1991: *Physicochemical and Environmental Plant Physiology.* Academic Press, 635 pp.

Ogink-Hendriks, M. J., 1995: Modelling surface conductance and transpiration of an oak forest in the Netherlands. *Agric. For. Meteor.,* **74,** 99–118.

Paw U, K. T., and Coauthors, 2004: Carbon dioxide exchange between an old growth forest and the atmosphere. *Ecosystems,* in press.

Sellers, P. J., and Coauthors, 1996: A revised land surface parameterization (SiB2) for atmospheric GCMs. Part I: Model formulation. *J. Climate,* **9,** 676–705.

——, and Coauthors, 1997: BOREAS in 1997: Experiment overview, scientific results, and future directions. *J. Geophys. Res.,* **102,** 28 731–28 769.

Shaw, D. C., J. F. Franklin, J. Klopatek, E. Freeman, K. Bible, T. Newton, S. Greene, and J. Wade-Murphy, 2004: Ecological setting of the Wind River old-growth forest. *Ecosystems,* in press.

Stewart, J. B., 1988: Modelling surface conductance of pine forest. *Agric. For. Meteor.,* **43,** 19–35.

Storck, P., L. Bowling, P. Wetherbee, and D. Lettenmaier, 1998: Application of a GIS-based distributed hydrology model for prediction of forest harvest effects on peak stream flow in the Pacific Northwest. *Hydrol. Processes,* **12,** 889–904.

——, D. P. Lettenmaier, and S. M. Bolton, 2002: Measurement of snow interception and canopy effects on snow accumulation and melt in a mountainous maritime climate, Oregon, United States. *Water. Resour. Res.,* **38,** 1223, doi:10.1029/2002WR001281.

Thomas, R. B., and W. F. Megahan, 1998: Peak flow responses to clear-cutting and roads in small and large basins, western Cascades, Oregon: A second opinion. *Water. Resour. Res.,* **34,** 3393–3403.

Thomas, S. C., and W. E. Winner, 2000: Leaf area index of an old-growth Douglas-fir forest estimated from direct structural measurements in the canopy. *Can. J. For. Res.,* **30,** 1922–1930.

Unsworth, M., and Coauthors, 2004: Components and controls of water flux in an old growth Douglas fir/western hemlock ecosystem. *Ecosystems,* in press.

U.S. Army Corps of Engineers, 1956: *Snow Hydrology: Summary Report of the Snow Investigations.* North Pacific Division, U.S. Army Corps of Engineers, 437 pp.

Wigmosta, M. S., L. W. Vail, and D. P. Lettenmaier, 1994: A distributed hydrology–vegetation model for complex terrain. *Water. Resour. Res.,* **30,** 1665–1679.

Williams, M., B. J. Bond, and M. G. Ryan, 2001: Evaluation of different soil and plant hydraulic constraints on tree function using a model and sap flow data from ponderosa pine. *Plant Cell Environ.,* **24,** 679–690.

Wilson, K. B., and Coauthors, 2002: Energy partitioning between latent and sensible heat flux during the warm season at FLUXNET sites. *Water. Resour. Res.,* **38,** 1294, doi:10.1029/2001WR000989.